

Analysis of the Genetic Characteristics and Metastatic Pathways of G1 and G2 Colorectal Neuroendocrine Neoplasms

Zhijie Wang,^{1,*} Qichen Chen,^{2,*} Fuqiang Zhao,^{3,*} Li Sun,⁴ Yixian Qiu,⁵ Huanqing Cheng,⁵ Jiayue Qin,⁵ Huina Wang,⁵ Susheng Shi,⁴ Shanbo Cao,⁵ and Qian Liu³

¹Key Laboratory of Carcinogenesis and Translational Research (Ministry of Education/Beijing), Department of Gastrointestinal Cancer Center, Peking University Cancer Hospital & Institute, Beijing 100142, China

²Department of Colorectal Surgery, State Key Laboratory of Oncology in South China, Guangdong Provincial Clinical Research Center for Cancer, Sun Yat-sen University Cancer Center, Guangzhou 510060, China

³Department of Colorectal Surgery, National Cancer Center/National Clinical Research Center for Cancer/Cancer Hospital, Chinese Academy of Medical Sciences and Peking Union Medical College, Beijing 100021, China

⁴Department of Pathology, National Cancer Center/National Clinical Research Center for Cancer/Cancer Hospital, Chinese Academy of Medical Sciences and Peking Union Medical College, Beijing 100021, China

⁵Acornmed Biotechnology Co., Ltd, Beijing 100176, China

Correspondence: Qian Liu, MD, Department of Colorectal Surgery, National Cancer Center/Cancer Hospital, Chinese Academy of Medical Sciences and Peking Union Medical College, No. 17, Panjiayuan Nanli, Chaoyang District, Beijing 100021, China. Email: qianliu_a123@163.com; or Shanbo Cao, PhD, Acornmed Biotechnology Co., Ltd, 18th Floor, Block 5, Yard 18, Kechuang 13 RD, Beijing 100176, China. Email: shanbocao@acornmed.com.

*These authors contributed equally to this work and share first authorship.

Abstract

Objective: G1 and G2 colorectal neuroendocrine neoplasms (NENs) are a group of rare and indolent diseases. We aimed to delineate their genetic characteristics and explore their metastatic mechanisms.

Methods: We used next-generation sequencing technology for targeted sequencing for 54 patients with G1 and G2 colorectal NENs. We delineated their genetic features and compared the genetic characteristics between metastatic NENs and nonmetastatic NENs. Kyoto Encyclopedia of Genes and Genomes (KEGG) enrichment analysis was utilized to explore their abnormal pathways and study their potential metastatic mechanisms.

Results: We collected 23 metastatic NENs and 31 nonmetastatic NENs. In the whole cohort, the common mutated genes were NCOR2, BRD4, MDC1, ARID1A, AXIN2, etc. The common copy number variations (CNVs) included amplification of HIST1H3D, amplification of HIST1H3E, and loss of PTEN. The KEGG enrichment analysis revealed that PI3K-Akt, MAPK, and Rap1 were the major abnormal pathways. There were significantly different genetic features between metastatic NENs and nonmetastatic NENs. The metastatic NENs shared only 47 (22.5%) mutated genes and 6 (13.3%) CNVs with nonmetastatic NENs. NCOR2, BRD4, CDKN1B, CYP3A5, and EIF1AX were the commonly mutated genes in metastatic NENs, while NCOR2, MDC1, AXIN2, PIK3C2G, and PTPRT were the commonly mutated genes in nonmetastatic NENs. Metastatic NENs presented a significantly higher proportion of abnormal pathways of cell senescence (56.5% vs 25.8%, $P = .022$) and lysine degradation (43.5% vs 16.1%, $P = .027$) than nonmetastatic NENs.

Conclusion: G1 and G2 colorectal NENs are a group of heterogeneous diseases that might obtain an increased invasive ability through aberrant cell senescence and lysine degradation pathways.

Key Words: colon, rectum, neuroendocrine, neoplasm, metastasis, genomics

Colorectal neuroendocrine neoplasms (NENs) are a group of rare diseases, but their incidence has been increasing in recent decades, possibly owing to the popularization of colonoscopy screening [1]. Based on the 2019 World Health Organization classification of tumors of the digestive system, colorectal NENs were classified into G1, G2, and G3 NENs. Specifically, poorly differentiated and grade G3 NENs are termed neuroendocrine carcinomas (NECs) [2]. However, G1 and G2 NENs are the most common and constitute 74.0% to 78.8% of all colorectal NENs [3, 4]. G1 and G2 colorectal NENs are often

characterized as a group of indolent diseases with low malignant potential and low aggressiveness, and most of them are found as diminutive lesions confined only in the mucosa and submucosa and need only local excision [5, 6]. However, some previous reports have shown that metastatic disease can still be found in the minority of G1 and G2 colorectal NENs. It has been found that 3.6% to 14.6% of them can show regional lymph node metastasis, and 0.8% to 8.5% of them can show distant metastasis [7–9]. Other case reports showed that some patients can present metastatic disease even when the maximal diameter of the lesion is less

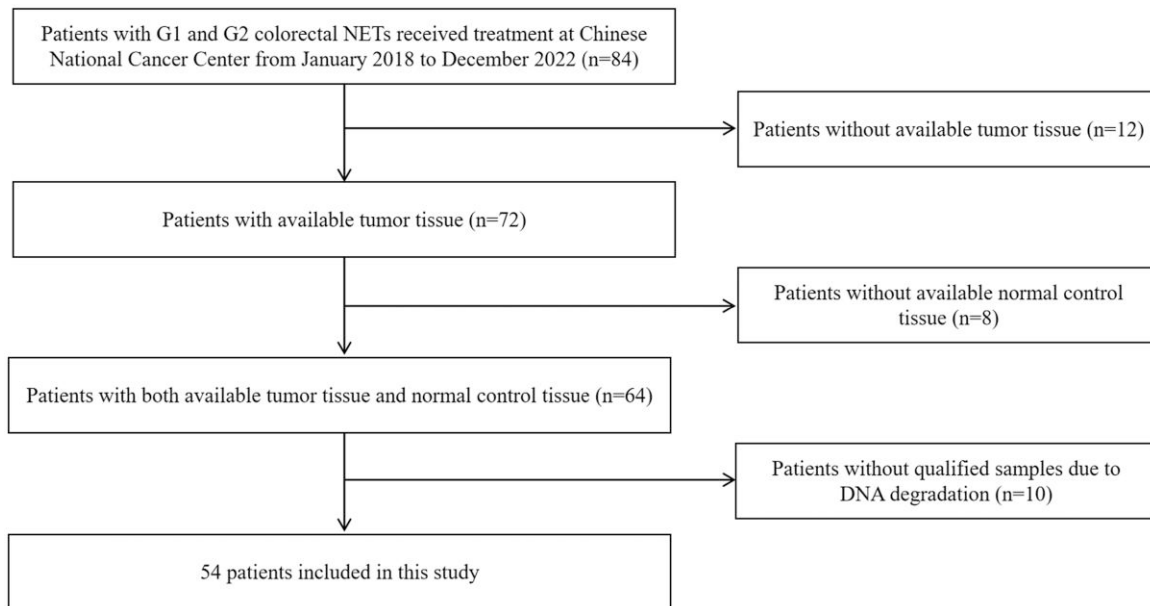


Figure 1. Flow chart presenting the patients' enrollment in our study.

than 10 mm, which has exceeded clinicians' foundational understanding of this disease [10-12].

Due to the low incidence of colorectal NENs, difficulty in sample collection, and lack of preclinical research platforms, the genetic characteristics of G1 and G2 colorectal NENs have not been fully delineated thus far. Moreover, no previous studies have explored their underlying metastatic mechanisms. All of these factors lead to very limited choices of chemotherapy drugs and regimens for these patients [3, 13]. Based on the limitations and lack of knowledge surrounding colorectal NENs, we aimed to explore the genomic characteristics, potential targetable gene alterations, and abnormal signaling pathways of G1 and G2 colorectal NENs. Moreover, we planned to compare the genetic differences between patients with metastatic disease and those without and intended to identify the underlying signal pathways of tumor spread.

Materials and Methods

Patients and Sample Collection

This study was approved by the Ethical Committee of the Chinese National Cancer Center and was conducted in accordance with the Declaration of Helsinki. The inclusion criteria were as follows: (1) all patients were pathologically diagnosed with NENs; (2) all NENs were confirmed as G1 or G2 NENs; (3) all NENs were located in the colon and rectum. Following our inclusion criteria, we identified a total of 84 patients with G1 and G2 colorectal NENs who received treatment at the Chinese National Cancer Center/Cancer Hospital Chinese Academy of Medical Sciences from January 2018 to December 2022, but only 54 of them were eligible for DNA sequencing and were ultimately included in the study (Fig. 1). The corresponding cancer tissue samples were collected, including 50 formalin-fixed paraffin embedding specimens and 4 fresh tissue samples. The corresponding matched normal tissue samples were also collected, including 46 tumor-adjacent tissues and 8 blood samples, which were sequenced to exclude germline variants. We defined regional lymph node metastasis or

distant metastasis as tumor metastasis; thus, 23 patients were categorized into the metastatic group and 31 patients were categorized into the nonmetastatic group.

DNA Extraction

DNA was extracted from the tissue using the QIAamp Genomic DNA kit (Qiagen GmbH). The quantification and quality of the DNA were assessed using a Qubit 2.0 fluorimeter with a dsDNA HS assay kit (Thermo Fisher Scientific, Inc.) and an Agilent 2100 BioAnalyzer (Agilent Technologies, Inc.), respectively. For blood samples, at least 10 mL of peripheral blood was collected and then centrifuged for 10 minutes (1600 revolutions per minute). After centrifugation, peripheral blood leukocytes were collected for genomic DNA extraction. DNA of peripheral blood leukocytes was extracted using the MagCore Genomic DNA Whole Blood Kit [Concert Biotechnology (Xiamen) Corp., China].

Library Construction and Targeted NGS

The sequencing libraries were generated according to the manufacturer's instructions (Illumina Inc). A total of 108 libraries were generated including 54 tumor tissue sequencing libraries and 54 matched control sequencing libraries. Targeted next-generation sequencing was performed at AcornMed Biotechnology (Beijing, China) using an Illumina HiSeq6000 platform (Illumina, San Diego, CA, USA). An 808 cancer-related gene panel targeting more than 2.0 Mb of the coding genome was detected for each case, which was enriched for the coding regions and selected introns of genes with known relevance to colorectal tumors. The sequencing depth was $>10\,000\times$. After the removal of the low-quality sequencing data, sequence reads were aligned to a human reference genome (hg19) by the Burrows-Wheeler alignment (version 0.7.12) tool. Local realignment and base quality score recalibration were conducted using GATK software (version 3.8). Single nucleotide variants and small insertions or deletions were analyzed using MuTect2 (version 1.1.7) with the recommended parameters. CNV calling was conducted with CONTRA software (version 2.0.8). Mutation spectrum analysis

was performed using the maftools package in R (version 4.1.2). OncoKB analysis was performed using MSK's Precision Oncology Knowledge Base (<https://www.oncokb.org/>), which classifies targetable mutations into 1 of 4 levels according to the strength of evidence supporting the use of certain drugs. InterVar software (v2.2.1) was used to categorize missense variants as benign/pathologic. Moreover, the genetic characteristics of colorectal adenocarcinomas discussed in this article were based on the American Association of Cancer Research Project Genomics, Evidence, Neoplasm, Information, Exchange database [14].

Statistical Analysis

The research data are presented as numbers with frequencies, and the differences between the groups were analyzed by the χ^2 test or Fisher's exact test. The overall survival (OS) rates and progression-free survival (PFS) rates were calculated through Kaplan–Meier curves and compared by log-rank test. Univariate and multivariate Cox regression analyses were performed to identify independent prognostic factors. Kyoto Encyclopedia of Genes and Genomes (KEGG) pathway enrichment analysis was performed to explore the abnormal pathways affected by mutant genes.

All tests were 2-sided, and $P < .05$ was considered statistically significant. All statistical analyses were performed using either the Statistical Package for the Social Sciences (SPSS version 24.0; IBM Corp., Armonk, NY, USA) or R software version 4.1.2 (<https://www.r-project.org/>).

Results

The Clinicopathological Features of Patients

The clinicopathological manifestations of the patients are shown in Table 1. In total, 54 eligible patients were included in our study; 23 patients suffered from metastatic disease, and the other 31 patients did not. Twenty-nine (53.7%) patients were male, and 43 patients were below 60 years old. The majority (92.6%) of patients had their tumors located in the rectum, and only 4 (7.4%) patients had their tumors located in the colon. Despite the absence of distant metastasis in the 4 patients with colonic NENs, 3 of them were categorized within the metastasis group due to the presence of concurrent regional lymph node metastasis. With regard to tumor size, 21 (38.9%) patients had tumors smaller than 1 cm, 19 (35.2%) had tumors 1 to 2 cm in size, and 14 (25.9%) had tumors 2 cm or larger in size. Regarding tumor grade, 34 (63.0%) patients had G1 NENs, and 20 (37.0%) patients had G2 NENs. Ten (18.5%) patients and 14 (25.9%) patients had lymphovascular invasion and perineural invasion, respectively. Of these patients, 25 (46.3%) received local excision, 27 (50%) underwent radical resection, and 2 (3.7%) received no surgical treatment due to widespread metastasis. With regard to the depth of tumor invasion, 37 (68.5%) invaded only the mucosa and submucosa, 11 (20.4%) invaded the muscularis propria, 4 (7.4%) infiltrated the subserosa, and 2 (3.7%) infiltrated the serosa. Twenty-three (42.6%) and 7 (13.0%) patients suffered regional lymph node metastasis and distant metastasis, respectively. The statistical analysis demonstrated that the metastatic group had a higher proportion of patients with larger tumor size ($P < .001$), G2 NENs ($P < .001$), lymphovascular invasion ($P = .022$), perineural invasion ($P < .001$), deeper depth of invasion ($P < .001$), regional

lymph node metastasis ($P < .001$), and distant metastasis ($P < .001$) than the nonmetastatic group.

Somatic Mutation Characteristics

In total, 38 (70.4%) patients had at least 1 mutated gene, and 209 genes with 355 mutation sites were detected, including 306 (86.2%) missense mutations, 17 (4.8%) frameshift mutations, 10 (2.8%) in-frame mutations, 15 (4.2%) splicing mutations, 6 (1.7%) nonsense mutations, and 1 (1.3%) mutation, which led to the loss of the termination codon. The top 50 high-frequency gene mutations are shown in Fig. 2. The common mutated genes were NCOR2 (24.1%), BRD4 (11.1%), MDC1 (11.1%), ARID1A (9.3%), AXIN2 (9.3%), CDKN1B (9.3%), KMT2D (9.3%), PTPRT (9.3%), etc. Subsequently, we analyzed the coexistence and mutual exclusiveness of the mutated genes (Fig. 3). We found that mutated NCOR2 significantly co-occurred with mutated CHEK2 ($P < .01$), ARID1A ($P < .05$), and MDC1 ($P < .05$). Moreover, coexistence of MDC1 and CHEK2 ($P < .05$) and coexistence of ARID1A and PTPRT ($P < .01$) were also observed.

The detection rates of gene mutations were 73.9% and 67.7% in the metastatic group and nonmetastatic group ($P = .623$), respectively. Significantly different somatic mutation characteristics were found between the 2 groups. In the metastatic group, the common mutated genes included NCOR2 (21.7%), BRD4 (13%), CDKN1B (13%), CYP3A5 (13%), EIF1AX (13%), ARID1A (8.7%), ATM (8.7%), EP300 (8.7%), FAT1 (8.7%), FGFR3 (8.7%), KIT (8.7%), and KMT2A (8.7%). In the nonmetastatic group, the common mutated genes included NCOR2 (25.8%), MDC1 (19.4%), AXIN2 (12.9%), PIK3C2G (12.9%), PTPRT (12.9%), ARID1A (9.7%), BRD4 (9.7%), CHEK2 (9.7%), FANCA (9.7%), FAT3 (9.7%), KMT2D (9.7%), MLXIPL (9.7%), PIK3C2B (9.7%), TSC2 (9.7%), etc. Mutations in ATM and KMT2A were found only in the metastatic group, and mutations in MDC1, PIK3C2G, FANCA, FAT3, MLXIPL, and PIK3C2B were observed only in the nonmetastatic group. The nonmetastatic group had a significantly higher mutation rate of MDC1 than the metastatic group (17.3% vs 0, $P = .030$). Of the 209 detected mutated genes, only 47 (22.5%) genes were found in both groups, and 73 (35.0%) and 89 (42.6%) genes were found only in the metastatic group and nonmetastatic group, respectively (Fig. 4A). In the 311 mutation sites, the metastatic group shared only 20 (6.4%) mutation sites with the nonmetastatic group, and 127 (40.8%) and 164 (52.7%) were detected only in the metastatic group and nonmetastatic group, respectively (Fig. 4B).

Characteristics of CNVs

In total, 19 (35.2%) patients were detected with CNVs, and 45 genes with 57 CNVs were found (Fig. 5). The common CNVs included amplification of HIST1H3D (5.6%) and HIST1H3E (5.6%) and loss of PTEN (5.6%). In the metastatic group, 10 (43.5%) patients carried 26 CNVs of 24 genes, including amplification of HIST1H3D (4.3%), HIST1H3E (4.3%), and BTG2 (4.3%) and loss of PTEN (8.7%), SMD2 (8.7%), ADGRG4 (4.3%), and FLT4 (4.3%). In the nonmetastatic group, 9 (29.0%) patients harbored 31 CNVs of 27 genes, including amplification of HIST1H3D (6.5%), HIST1H3E (6.5%), and BTG2 (3.2%) and loss of PTPRT (6.5%), PTEN (3.2%), ADGRG4 (3.2%), and FLT4 (3.2%). Both the amplification and loss of BRCA1 were detected in the nonmetastatic group. There was a significant difference in CNV distribution

Table 1. The clinical and pathological features of patients

Variable	All (n = 54)	Nonmetastatic group (n = 31)	Metastatic group (n = 23)	P
Sex (%)				.583
Male	29 (53.7)	18 (58.1)	11 (47.8)	
Female	25 (46.3)	13 (41.9)	12 (52.2)	
Age (%)				1
<60	43 (79.6)	25 (80.6)	18 (78.3)	
≥60	11 (20.4)	6 (19.4)	5 (21.7)	
Tumor location (%)				.403
Colon	4 (7.4)	1 (3.2)	3 (13)	
Rectum	50 (92.6)	30 (96.8)	20 (87)	
Tumor size (cm) (%)				<.001
<1	21 (38.9)	19 (61.3)	2 (8.7)	
1–2	19 (35.2)	11 (35.5)	8 (34.8)	
≥2	14 (25.9)	1 (3.2)	13 (56.5)	
Tumor grade (%)				<.001
G1	34 (63.0)	28 (90.3)	6 (26.1)	
G2	20 (37.0)	3 (9.7)	17 (73.9)	
Lymphovascular invasion (%)				.022
Positive	10 (18.5)	2 (6.5)	8 (34.8)	
Negative	44 (81.5)	29 (93.5)	15 (65.2)	
perineural invasion (%)				<.001
Positive	14 (25.9)	2 (6.5)	12 (52.2)	
Negative	40 (74.1)	29 (93.5)	11 (47.8)	
Surgery (%)				<.001
Local excision	25 (46.3)	25 (80.6)	0	
Radical resection	27 (50)	6 (19.4)	21 (91.3)	
vs no surgery	2 (3.7)	0	2 (8.7)	
Depth of the invasion (%)				<.001
Mucosa and submucosa	37 (68.5)	29 (93.5)	8 (34.8)	
Muscularis propria	11 (20.4)	2 (6.5)	9 (39.1)	
Subserosa	4 (7.4)	0	4 (17.4)	
Serosa	2 (3.7)	0	2 (8.7)	
Nodal metastasis (%)				<.001
Positive	23 (42.6)	0	23 (100)	
Negative	31 (57.4)	31 (100)	0	
Distant metastasis (%)				.004
Positive	7 (13.0)	0	7 (30.4)	
Negative	47 (87.0)	31 (100)	16 (69.6)	
TNM staging (%)				<.001
I	29 (53.7)	29 (93.5)	0	
II	2 (3.7)	2 (6.5)	0	
III	16 (29.6)	0	16 (69.6)	
IV	7 (13.0)	0	7 (30.4)	

between the 2 groups. Of the 45 genes with CNVs, only 6 (13.3%) genes were observed in both groups, and 18 (40.0%) and 21 (46.7%) genes were found only in the metastatic group and nonmetastatic group, respectively (Fig. 4C).

Mutation Spectrum and Mutation Signature Analysis

The mutation spectrum analysis showed that C > T and T > C transitions were the major fractions of base substitutions in

G1 and G2 colorectal NENs. Base transition was much more frequent than base transversion (Fig. 6A). Following mutation signature analysis of 96 substitution patterns using the non-negative matrix factorization algorithm, 5 mutation signatures were identified in G1 and G2 colorectal NENs. Subsequently, we tried to match the 5 mutation signatures with the acknowledged mutation signatures previously recorded in the COSMIC database [15]. We found that signature B, which was characterized by a dominant T > G

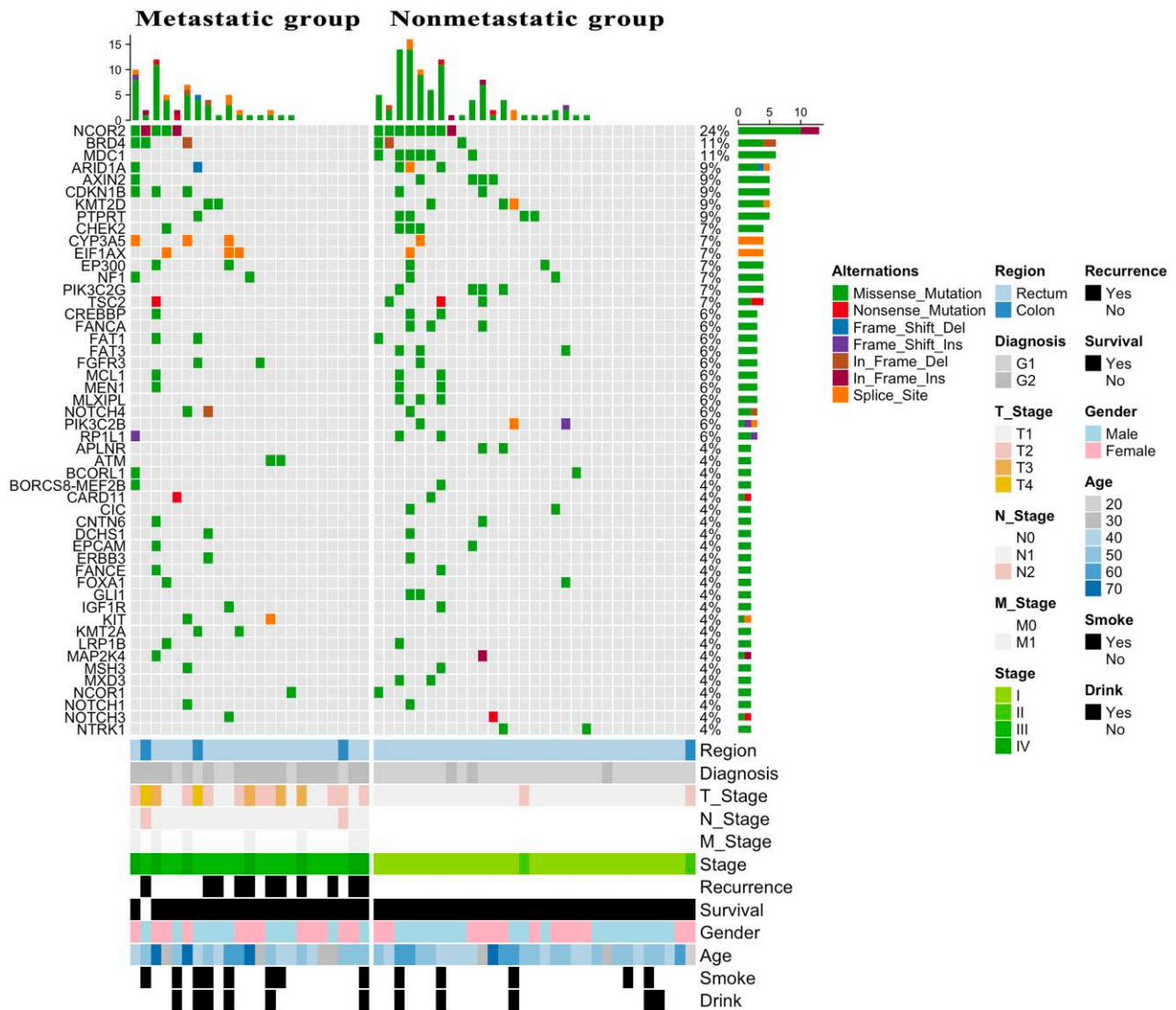


Figure 2. Top 50 genes with somatic mutation in G1 and G2 colorectal neuroendocrine neoplasms.

transition, was highly similar to signature 17 (cosine correlation similarity = 0.75), and signature C, which was characterized by a dominant C > T transition, was consistent with signature 1 (cosine correlation similarity = 0.85) (Fig. 6B).

Integration of Altered Pathways in G1 and G2 Colorectal NENs

We performed KEGG enrichment analysis based on the detected mutated genes (Fig. 7). The PI3K-AKT ($P < .001$), MAPK ($P < .001$), Rap1 ($P < .001$), RAS ($P < .001$), FoXO ($P < .001$), and cellular senescence ($P < .001$) pathways were commonly altered by gene mutations. The PI3K-AKT signaling pathway was altered in 44.4% of all patients, and cellular senescence and the FoXO signaling pathway were affected in 38.9% of all patients. Subsequently, we explored the difference between the metastatic group and the nonmetastatic group. In the metastatic group, the most common abnormal pathway was cellular senescence, which was affected in 56.5% of patients. The PI3K-AKT signaling pathway was mostly altered in the nonmetastatic group and was altered in 45.2% of patients. The frequencies of altered cellular

senescence (56.5% vs 25.8%, $P = .022$) and lysine degradation (43.5% vs 16.1%, $P = .027$) in the metastatic group were significantly higher than those in the nonmetastatic group (Fig. 8).

Potential Targetable Gene Mutations Annotated Using OncoKB

In total, 24 (44.4%) patients with 26 potential targetable gene mutations in the whole cohort were detected, including ARID1A (9.3%), CHEK2 (7.4%), NF1 (7.4%), and TSC2 (7.4%) (Fig. 9). In the metastatic group, 12 (52.2%) patients with 21 potential targetable gene mutations were found, including 16 mutations of level 1, 2 mutations of level 3A, and 3 mutations of level 4. In the nonmetastatic group, 12 (39.7%) patients with 14 potential targetable gene mutations were found, including 12 mutations of level 1 and 2 mutations of level 4.

Our study found 6 (11.1%) patients with 5 potential targetable CNVs in the entire cohort (Fig. 9). In the metastatic group, 3 (12.5%) patients harbored potential targetable CNVs, including loss of PIK3CA (level 1), FGFR2 (level 1), and PTEN (level 4). In the metastatic group, 3 (9.7%) patients

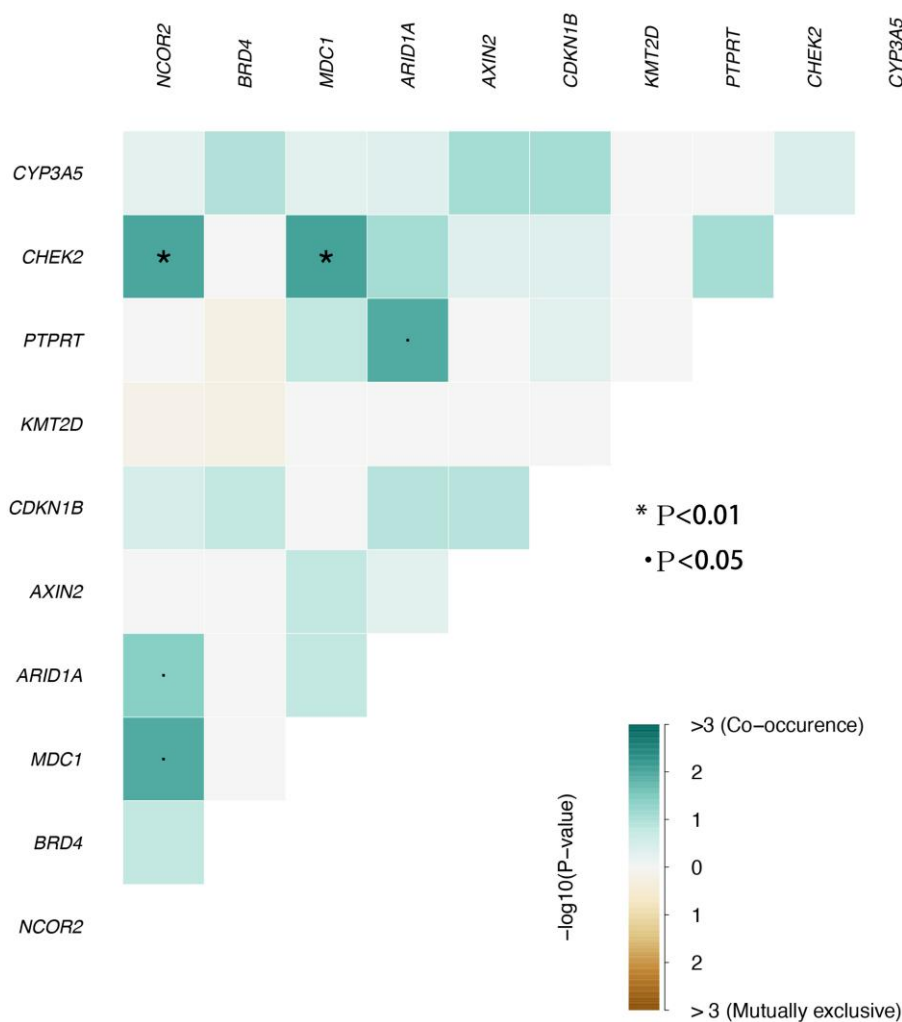


Figure 3. The coexistent mutated genes in G1 and G2 colorectal neuroendocrine neoplasms.

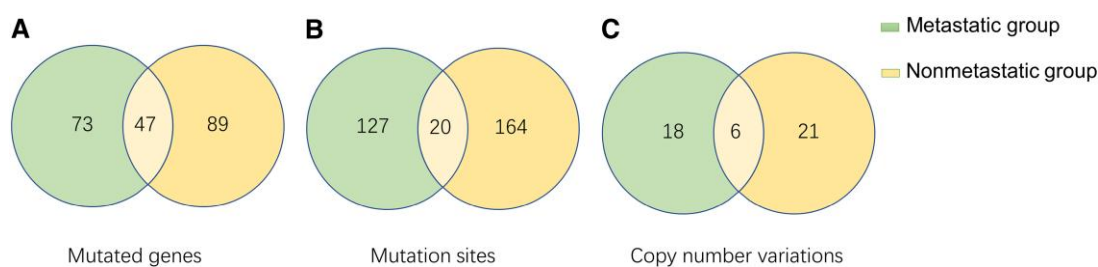


Figure 4. Frequencies of exclusive and shared gene alterations as indicated by Venn diagrams. (A) Mutated genes; (B) mutation sites; (C) copy number variations.

harbored potential targetable CNVs, including amplification of BRCA1 (level 1) and CDK4 (level 4) and loss of BRCA1 (level 1) and PTEN (level 4).

Gene Alteration and Survival

All patients were followed up for a median duration of 27 months (range 14–71 months), and no patients were lost to follow-up. During the follow-up, 11 patients suffered from tumor progression, and only 1 patient died from tumor progression. In the nonmetastatic group, the 1-year and 3-year PFS

rates were both 100%. In the metastatic group, the 1-year and 3-year PFS rates were 73.9% and 53.4%, respectively (Fig. 10A). The metastatic group presented significantly worse PFS than the nonmetastatic group ($P < .001$). The 1-year OS rates were both 100% in the 2 groups, while the 3-year OS rates were 92.3% in the metastatic group and 100% in the nonmetastatic group, which was not significantly different ($P = .267$, Fig. 10B). Furthermore, patients with KMT2D mutations showed a significantly higher risk of tumor progression than those without KMT2D mutations ($P = .045$, Fig. 10C). The multivariate Cox regression analyses also confirmed that

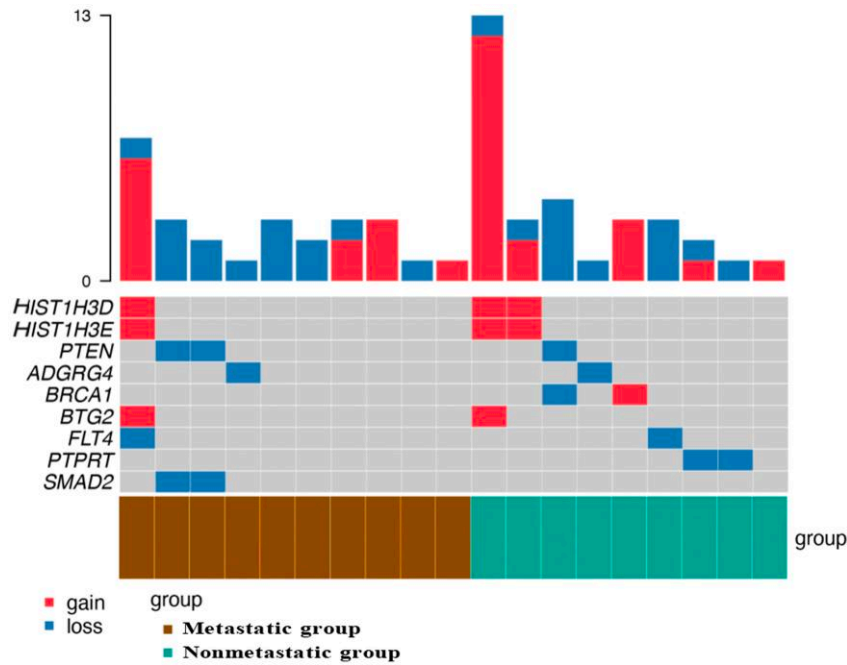


Figure 5. The top 10 genes with copy number variations in G1 and G2 colorectal neuroendocrine neoplasms.

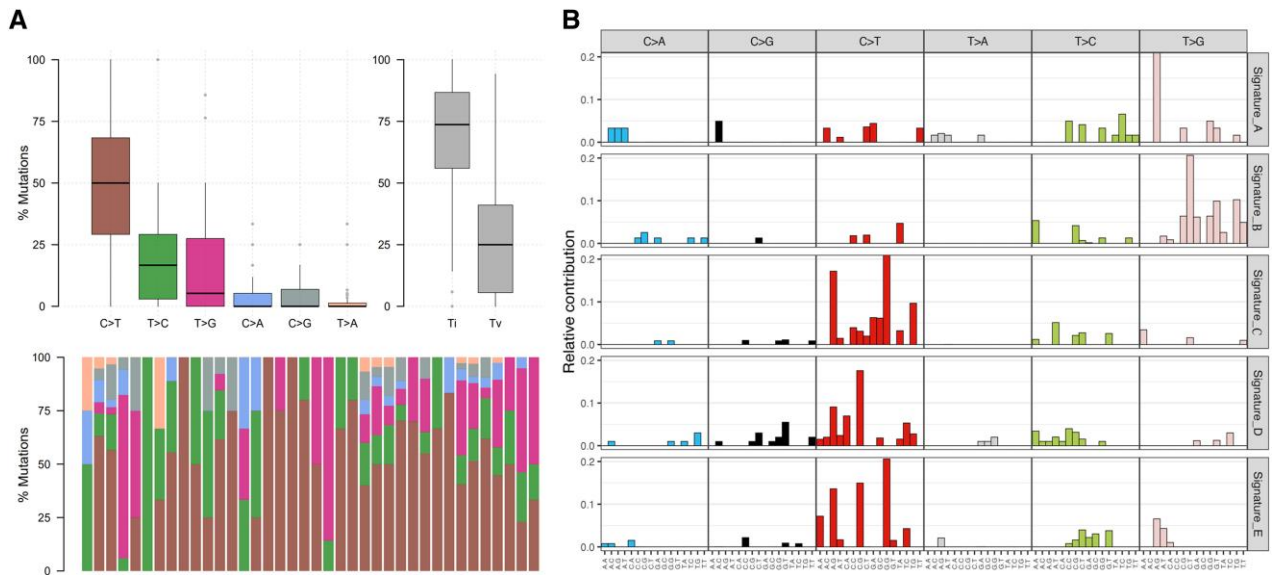


Figure 6. The mutation spectrum and mutation signatures in G1 and G2 colorectal neuroendocrine neoplasms. (A) Mutation spectrum; (B) mutation signatures.

KMT2D mutation [hazard ratio = 13.301, 95% confidence interval: 1.644–107.626, $P = .015$) was an independent risk factor for tumor progression in G1 and G2 colorectal NENs (Table 2).

Discussion

Colorectal NENs are a group of diseases with high heterogeneity. Previous DNA sequencing studies have focused mainly on colorectal NECs, and few studies have reported the genomic characteristics of G1 and G2 colorectal NENs. Our study indicated that G1 and G2 colorectal NENs had significantly

different genetic features from colorectal NECs. Colorectal NECs had similar gene mutations to colorectal adenocarcinomas, including TP53 (24%-65.5%), APC (16%-59.5%), KRAS (24%-36.9%), BRAF (20.2%-44.4%), and RB1 (4%-16.7%) [14, 16, 17]. However, these gene alterations were rarely found in G1 and G2 colorectal NENs, and only BRAF mutations (1.9%) and RB1 mutations (1.9%) were detected in one patient. Unlike BRAF V600E in exon 15, which is common in colorectal adenocarcinomas and NECs, the mutation site was in exon 1 (c.64G > A; p. D22N) in G1 and G2 colorectal NENs. Our study demonstrated that NCOR2 (24.1%), BRD4 (11.1%), MDC1 (11.1%), ARID1A (9.3%), and

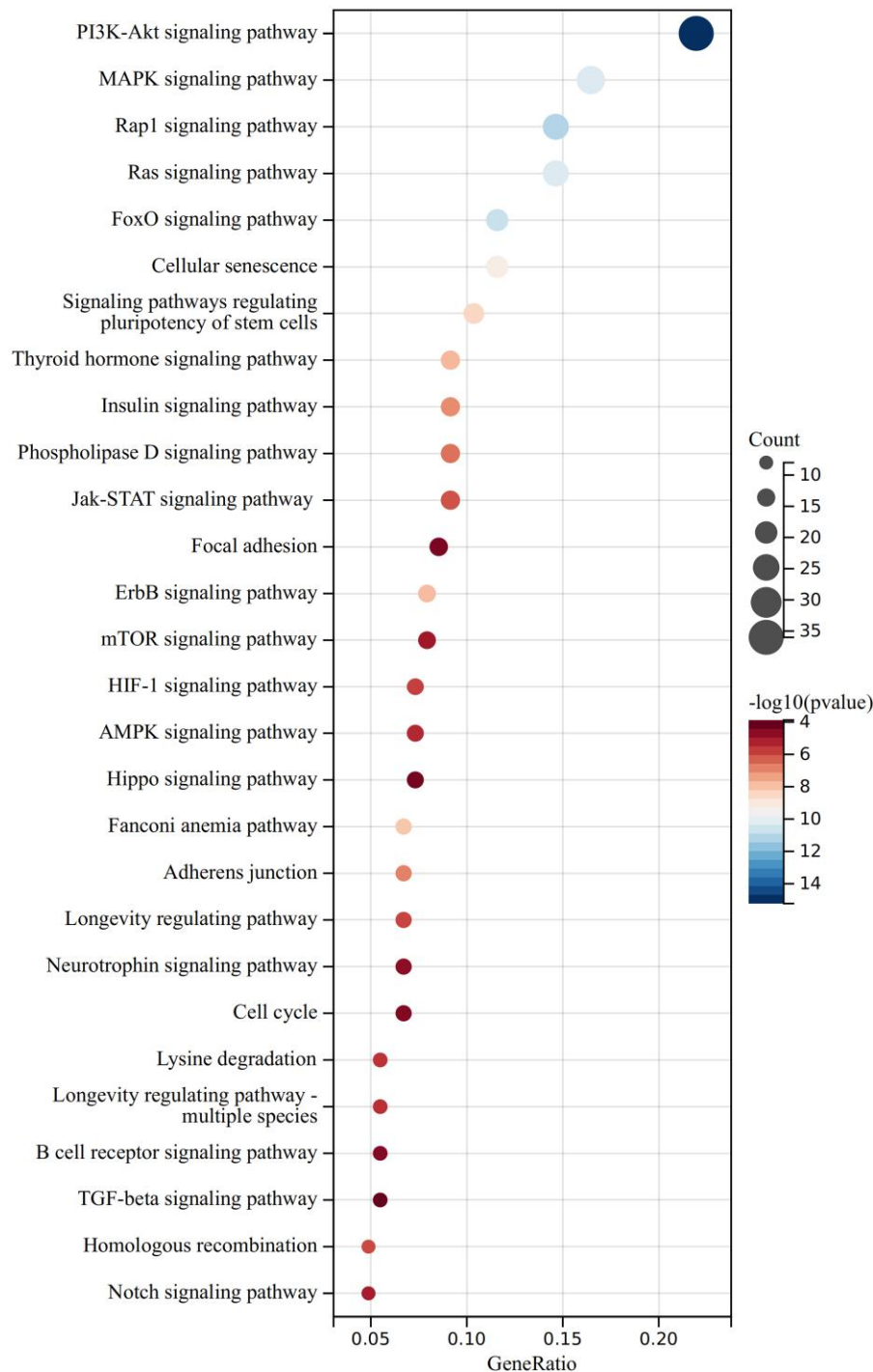


Figure 7. The abnormal pathways affected by mutated genes in G1 and G2 colorectal neuroendocrine neoplasms following KEGG enrichment analysis. Abbreviations: KEGG, Kyoto Encyclopedia of Genes and Genomes.

AXIN2 (9.3%) were the common mutated genes in G1 and G2 colorectal NENs. Previous reports showed that the common CNVs in colorectal NECs included amplification of MYC and loss of RB1 (10.7%) and PTEN (5.4%). However, neither the CNVs of MYC nor RB1 were found in G1 and G2 colorectal NENs, and only loss of PTEN was detected in 5.6% in our study.

KEGG enrichment analysis showed that the PI3K-AKT, cellular senescence, MAPK, and FoXO pathways were frequently altered by mutated genes in G1 and G2 colorectal NENs.

Only abnormal PI3K-AKT and MAPK pathways were also reported in colorectal NECs in previous studies, and cellular senescence and FoXO pathways were rarely altered in colorectal NECs [14]. Moreover, we found that only 44.4% of G1 and G2 colorectal NENs harbored potential targetable mutated genes, which was much lower than colorectal NECs. Previous sequencing studies showed that 76.7% of colorectal NECs harbored potential targetable mutated genes, and the common potential targetable mutated genes were similar to colorectal adenocarcinomas, including KRAS and

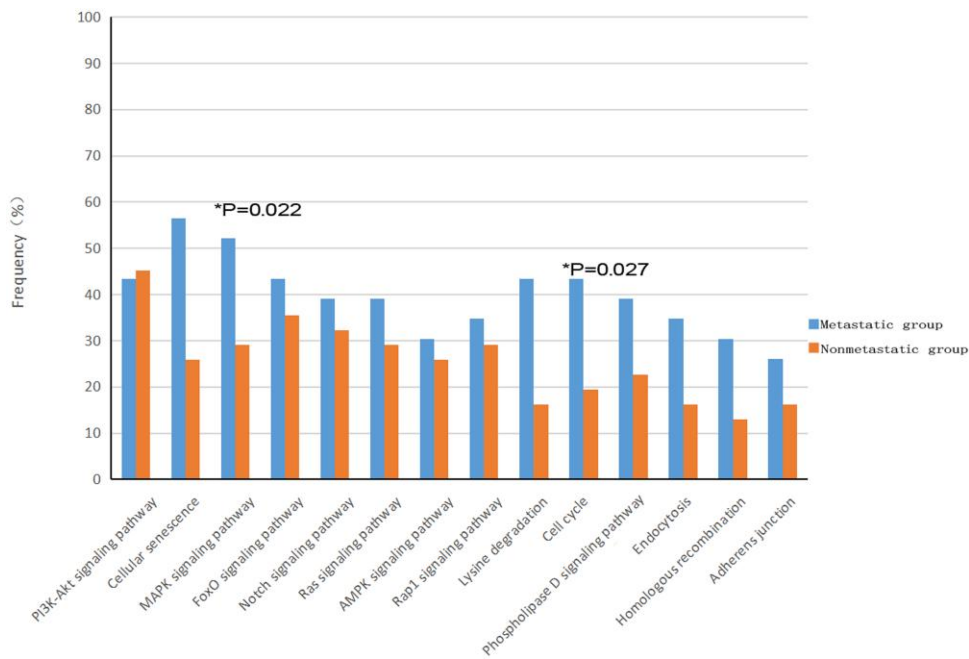


Figure 8. The frequency differences of abnormal pathways between metastatic group and nonmetastatic group in G1 and G2 colorectal neuroendocrine neoplasms.

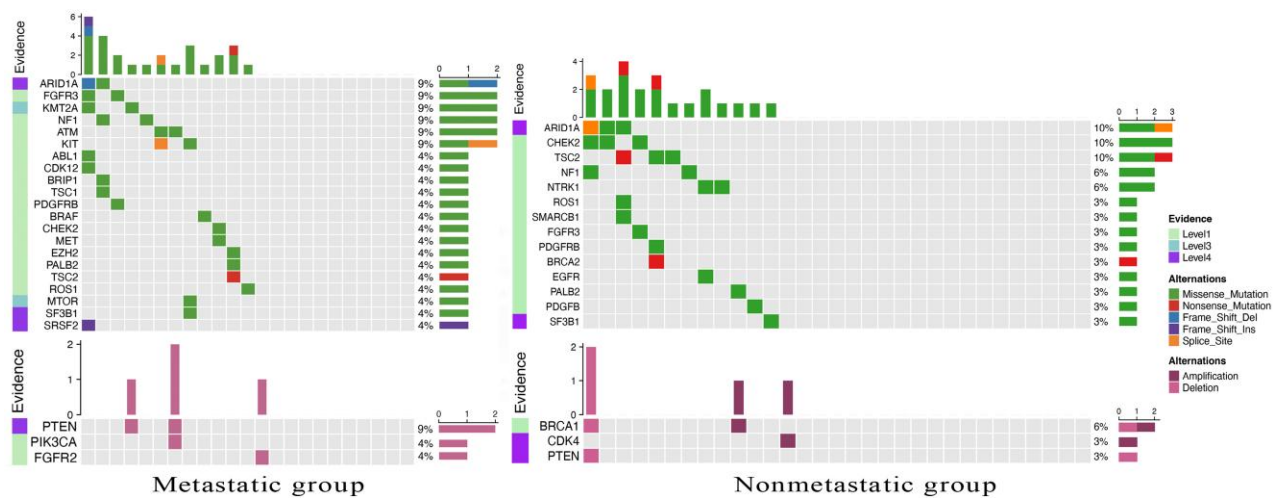


Figure 9. Potentially actionable gene alterations for targeted therapy in G1 and G2 colorectal neuroendocrine neoplasms.

BRAF [14, 18, 19]. The common potential targetable mutated genes in G1 and G2 colorectal NENs included ARID1A, CHEK2, NF1, TSC2, TSC1, and MTOR, and these mutated genes often led to abnormal MAPK, RAS, PI3K-AKT, and mTOR signaling pathways. TSC1, TSC2, and MTOR were the targets of everolimus in renal cell carcinoma, bladder cancer, and encapsulated glioma [20]. Everolimus is a type of mTOR inhibitor that has been used to treat well-differentiated digestive NENs and has presented favorable antitumor efficacy. At present, everolimus has been approved by the Food and Drug Administration to treat well-differentiated pancreatic NENs [21, 22]. Our study indicated that everolimus might be a candidate for targeted therapy in G1 and G2 colorectal NENs.

The previous mutation spectrum analysis showed that C > T and T > C transitions were the major fractions of mutations, and signature 1, signature 3, signature 5, and signature 15 were the main mutation signatures in colorectal NENs [23, 24]. Our findings were in line with previous reports, and signature 1 and signature 17 were identified in our study. Signature 1 was the result of an endogenous mutational process initiated by spontaneous deamination of 5-methylcytosine and correlated with age at cancer diagnosis [15]. This signified that the pathogenesis of G1 and G2 colorectal NENs increased with age and lacked carcinogen exposure. Our study first found signature 17 in G1 and G2 colorectal NENs, but the etiology of signature 17 remains unknown thus far.

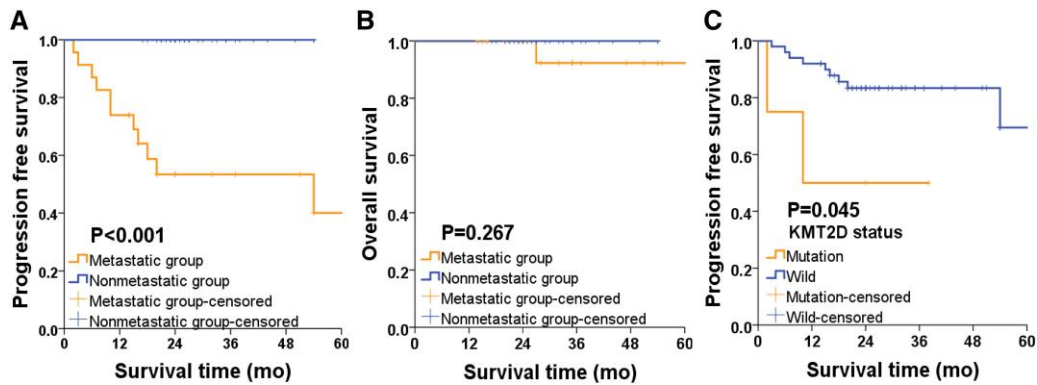


Figure 10. Kaplan–Meier curves in G1 and G2 colorectal neuroendocrine neoplasms. (A) PFS between metastatic group (n = 23) and nonmetastatic group (n = 31); (B) OS between metastatic group (n = 23) and nonmetastatic group (n = 31); (C) PFS between patients with mutated KMT2D (n = 5) and patients with wild KMT2D (n = 49).

Abbreviations: OS, overall survival; PFS, progression-free survival.

Table 2. Univariate and multivariate cox regression analysis of PFS

	Univariate analysis		Multivariate analysis	
	HR (95% CI)	P	HR (95% CI)	P
Sex	0.576 (0.167–1.984)	0.382		
Age	1.022 (0.973–1.075)	0.381		
Tumor size	1.939 (1.389–2.707)	<0.001	1.284 (0.533–3.094)	.578
Tumor location	1.167 (0.147–9.230)	0.884		
Tumor grade	20.201 (2.570–158.785)	0.004	9.683 (0.721–130.018)	.087
T stage				
T1	1			
T2	8.868 (1.706–46.100)	0.009	2.656 (0.405–17.436)	.309
T3	22.759 (3.722–139.172)	0.001	4.570 (0.398–52.503)	.223
T4	14.420 (1.288–161.449)	0.030	7.095 (0.060–839.353)	.421
NCOR mutation	0.325 (0.042–2.541)	0.284		
BRD4 mutation	0.880 (0.111–6.948)	0.903		
KMT2A mutation	2.905 (0.367–23.007)	0.312		
KMT2D mutation	4.290 (0.908–20.272)	0.066	13.301 (1.644–107.626)	.015
KIT mutation	4.097 (0.515–32.590)	0.183		
ATM mutation	10.587 (2.173–51.581)	0.003	1.916 (0.149–24.602)	.618

Abbreviations: CI, confidence interval; HR, hazard ratio; PFS, progression-free survival.

For a long time, G1 and G2 colorectal NENs were regarded as a type of benign disease by most physicians owing to their indolent nature. However, metastatic disease was indeed reported in G1 and G2 colorectal NENs in many previous reports [25]. We found that there were significantly different genetic characteristics between patients with metastatic disease and those without. The mutually mutated genes, mutation sites and CNVs of the 2 groups occupied only minor fractions of all detected gene alterations. Based on the mutated genes found in the metastatic group and nonmetastatic group, we found that the cellular senescence pathway was mostly altered in metastatic patients and that the PI3K-AKT signaling pathway was mostly altered in nonmetastatic patients. The proportion of patients with abnormal cellular senescence and lysine degradation signaling pathways in the metastatic group was significantly higher than that in the nonmetastatic group.

Previous studies have shown that cell senescence and lysine degradation are closely related to tumor cell invasion and

metastasis, and the interaction between senescent cells and non-senescent cancer cells and lysine degradation products can enhance tumor cell invasion [26, 27]. Tumor cells can escape apoptosis through cell cycle arrest induced by cell senescence, and senescent cells can secrete cytokines termed senescence-associated secretory phenotype factors, including IL-1 α , IL-6, IL8, and TGF β . These senescence-associated secretory phenotypes can promote tumor cell migration and metastasis through epithelial-to-mesenchymal transition [28, 29]. Moreover, aging tumor cells can recruit specialized macrophages to promote the production of blood vessels and lymph vessels, providing other tumor cells with oxygen and nutrients, which can in turn promote tumor growth and metastasis [30, 31]. Milanovic et al found that some senescent tumor cells can acquire stem cell properties, and the acquisition of tumor stem cell properties can also promote the proliferation and invasion ability of tumor cells [32]. Wang et al found that CCNB2 can promote the aging of glioma cells and thus enhance their invasion and metastasis abilities

[33]. Ibrahim-Hashim et al found that free lysine can reduce the acidity of the prostate cancer cell microenvironment and inhibit its metastasis [34]. Wu et al found that thrombopoietin could drive colorectal cancer CD110+ tumor-initiating cells to develop liver metastasis by activating lysine degradation. Acetyl-CoA produced by lysine degradation can trigger tyrosine phosphorylation of LPR6 and finally activate Wnt signaling to promote CD110+ tumor-initiating cell self-renewal. Glutamic acid produced by lysine catabolism can regulate the redox status of CD110+ tumor-initiating cells, promoting their colonization and resistance in the liver. Based on these previous reports, we speculated that metastatic G1 and G2 colorectal NENs might exhibit increased tumor migration and metastasis abilities through abnormal cellular senescence and lysine degradation pathways compared with nonmetastatic G1 and G2 colorectal NENs.

Our study has the following limitations. First, we were unable to compare the genetic characteristics differences between colon and rectal NENs, as only 4 cases of colonic NENs patients were included in the study. Second, Ki67 labeling index values that were associated with metastases were not used in the survival analysis. Third, due to the inclusion of cases solely from the Chinese National Cancer Center and the higher proportion of patients with metastatic colorectal NENs treated at this center compared to other hospitals, selection bias was unavoidable. This has resulted in a higher proportion of metastatic lesions in this study compared to the literature. Fourth, G3 neuroendocrine tumors and NECs were not included in the study.

Conclusions

In conclusion, G1 and G2 colorectal NENs have significantly different genetic characteristics from colorectal NECs and adenocarcinomas. In G1 and G2 colorectal NENs, there may be a small subgroup known as metastatic NENs that exhibit significantly distinct genomic features compared to the majority of G1 and G2 colorectal NENs. They may acquire enhanced cell invasion and migration abilities through aberrant cellular senescence and lysine degradation pathways, which may lead to regional lymph node metastasis or distant metastasis of G1 and G2 colorectal NENs.

Acknowledgments

We acknowledge American Journal Experts for their language editing service for this manuscript.

Funding

This study is supported by the following grants: the National Key Research and Development Program (No.2022YFC2505003) and the CAMS Innovation Fund for Medical Sciences (No. 2022-12M-C&T-B-057).

Disclosures

The authors have no conflict of interest.

Data Availability

Some or all datasets generated during and/or analyzed during the current study are not publicly available but are available from the corresponding author on reasonable request.

References

1. Kooyker AI, Verbeek WH, van den Berg JG, Tesselaar ME, van Leerdam ME. Change in incidence, characteristics and management of colorectal neuroendocrine tumours in The Netherlands in the last decade. *United European Gastroenterol J*. 2020;8(1):59-67.
2. Nagtegaal ID, Odze RD, Klimstra D, et al. The 2019 WHO classification of tumours of the digestive system. *Histopathology*. 2020;76(2):182-188.
3. Xiao K, Zhao Y, Cai Y, et al. The effect of marital status on the survival of patients with colorectal neuroendocrine neoplasms: an analysis of the SEER database. *Rev Esp Enferm Dig*. 2020;112(2):109-117.
4. Ding X, Tian S, Hu J, et al. Risk and prognostic nomograms for colorectal neuroendocrine neoplasm with liver metastasis: a population-based study. *Int J Colorectal Dis*. 2021;36(9):1915-1927.
5. Hrabe J. Neuroendocrine tumors of the appendix, colon, and rectum. *Surg Oncol Clin N Am*. 2020;29(2):267-279.
6. Moon CM, Huh KC, Jung SA, et al. Long-term clinical outcomes of rectal neuroendocrine tumors according to the pathologic status after initial endoscopic resection: a KASID multicenter study. *Am J Gastroenterol*. 2016;111(9):1276-1285.
7. Folkert IW, Sinnamon AJ, Concors SJ, et al. Grade is a dominant risk factor for metastasis in patients with rectal neuroendocrine tumors. *Ann Surg Oncol*. 2020;27(3):855-863.
8. Yamaguchi T, Takahashi K, Yamada K, et al. A nationwide, multi-institutional collaborative retrospective study of colorectal neuroendocrine tumors in Japan. *Ann Gastroenterol Surg*. 2021;5(2):215-220.
9. Sekiguchi M, Hotta K, Takeuchi Y, et al. Characteristics of colorectal neuroendocrine tumors in patients prospectively enrolled in a Japanese multicenter study: a first report from the C-NET STUDY. *J Gastroenterol*. 2022;57(8):547-558.
10. Tsuboi K, Shimura T, Suzuki H, et al. Liver metastases of a minute rectal carcinoid less than 5mm in diameter: a case report. *Hepatogastroenterology*. 2004;51(59):1330-1332.
11. Shinohara T, Hotta K, Oyama T. Rectal carcinoid tumor, 6mm in diameter, with lymph node metastases. *Endoscopy*. 2008;40(Suppl 2):E40-E41.
12. Saito T, Ikenaga M, Yasui M, et al. A case of 7mm rectal carcinoid with lymph node metastasis. *Gan To Kagaku Ryoho*. 2009;36(12):2251-2253.
13. Chauhan A, Kohn E, Del Rivero J. Neuroendocrine tumors-less well known, often misunderstood, and rapidly growing in incidence. *JAMA Oncol*. 2020;6(1):21-22.
14. Chen L, Liu M, Zhang Y, Guo Y, Chen MH, Chen J. Genetic characteristics of colorectal neuroendocrine carcinoma: more similar to colorectal adenocarcinoma. *Clin Colorectal Cancer*. 2021;20(2):177-185.e113.
15. Alexandrov LB, Nik-Zainal S, Wedge DC, et al. Signatures of mutational processes in human cancer. *Nature*. 2013;500(7463):415-421.
16. Idrees K, Padmanabhan C, Liu E, et al. Frequent BRAF mutations suggest a novel oncogenic driver in colonic neuroendocrine carcinoma. *J Surg Oncol*. 2018;117(2):284-289.
17. Chen D, Bao X, Zhang R, et al. Depiction of the genomic and genetic landscape identifies CCL5 as a protective factor in colorectal neuroendocrine carcinoma. *Br J Cancer*. 2021;125(7):994-1002.
18. Dizdar L, Werner TA, Drusenheimer JC, et al. BRAF(v600e) mutation: a promising target in colorectal neuroendocrine carcinoma. *Int J Cancer*. 2019;144(6):1379-1390.
19. Nakano M, Shimada Y, Matsumoto Y, et al. Efficacy of BRAF inhibitor and anti-EGFR antibody in colorectal neuroendocrine carcinoma. *Clin J Gastroenterol*. 2022;15(2):413-418.
20. Devarakonda S, Pellini B, Verghese L, et al. A phase II study of everolimus in patients with advanced solid malignancies with TSC1, TSC2, NF1, NF2 or STK11 mutations. *J Thorac Dis*. 2021;13(7):4054-4062.
21. Yao JC, Fazio N, Singh S, et al. Everolimus for the treatment of advanced, non-functional neuroendocrine tumours of the lung or

- gastrointestinal tract (RADIA-4): a randomised, placebo-controlled, phase 3 study. *Lancet*. 2016;387(10022):968-977.
22. Pavel M, Oberg K, Falconi M, *et al*. Gastroenteropancreatic neuroendocrine neoplasms: ESMO clinical practice guidelines for diagnosis, treatment and follow-up. *Ann Oncol*. 2020;31(7):844-860.
 23. Wang TT, Lu J, Xu L, *et al*. Whole genome sequencing of colorectal neuroendocrine tumors and in-depth mutational analyses. *Med Oncol*. 2020;37(6):56.
 24. Li Y, Guo Y, Cheng Z, *et al*. Whole-exome sequencing of rectal neuroendocrine tumors. *Endocr Relat Cancer*. 2023;30(9):e220257.
 25. Wang Z, Liu Q. Development of novel prediction models for nodal and distant metastasis in G1 and G2 colorectal neuroendocrine tumors. *Int J Colorectal Dis*. 2023;38(1):37.
 26. Wu Z, Wei D, Gao W, *et al*. TPO-induced metabolic reprogramming drives liver metastasis of colorectal cancer CD110+ tumor-initiating cells. *Cell Stem Cell*. 2015;17(1):47-59.
 27. Takasugi M, Yoshida Y, Hara E, Ohtani N. The role of cellular senescence and SASP in tumour microenvironment. *FEBS J*. 2023;290(5):1348-1361.
 28. Hanahan D, Weinberg RA. Hallmarks of cancer: the next generation. *Cell*. 2011;144(5):646-674.
 29. Tesi A, Arienti C, Bossi G, *et al*. TP53 drives abscopal effect by secretion of senescence-associated molecular signals in non-small cell lung cancer. *J Exp Clin Cancer Res*. 2021;40(1):89.
 30. Qian BZ, Pollard JW. Macrophage diversity enhances tumor progression and metastasis. *Cell*. 2010;141(1):39-51.
 31. Yang H, Kim C, Kim MJ, *et al*. Soluble vascular endothelial growth factor receptor-3 suppresses lymphangiogenesis and lymphatic metastasis in bladder cancer. *Mol Cancer*. 2011;10(1):36.
 32. Milanovic M, Fan DNY, Belenki D, *et al*. Senescence-associated reprogramming promotes cancer stemness. *Nature*. 2018;553(7686):96-100.
 33. Wang Y, Zhang H, Wang M, *et al*. CCNB2/SASP/cathepsin b & PGE2 axis induce cell senescence mediated malignant transformation. *Int J Biol Sci*. 2021;17(13):3538-3553.
 34. Ibrahim-Hashim A, Wojtkowiak JW, de Lourdes Coelho Ribeiro M, *et al* Free base lysine increases survival and reduces metastasis in prostate cancer model. *J Cancer Sci Ther*. 2011; Suppl 1(4): JCST-S1-004.